

RESEARCH ARTICLE

# Uncertainty-Aware Matrix-Tolerance Decision Model for Direct and Automated Iron Isotope Analysis by Nitrogen-Plasma MC-MICAP-MS

David H. Waldeck<sup>1\*</sup>

<sup>1</sup>University of Pittsburgh

\*Corresponding author

Corresponding author:  
dave@pitt.edu



Received: 11 December 2025

Accepted: 22 February 2026

Available online: 30 March 2026

## Abstract

High-precision Fe isotope abundance ratios find wide application in environmental geochemistry, isotope metallomics, bioarchaeology, and biomedical research, since the slightest deviation of  $^{56}\text{Fe}/^{54}\text{Fe}$  and  $^{57}\text{Fe}/^{54}\text{Fe}$  can provide information on their source, processing, or physiology. However, the routine adoption of high-precision Fe isotope ratio measurements is currently limited by spectrally related interferences, matrix-related mass biases, procedural blanks, incomplete recovery, and the lengthy procedure involved in the chromatographic purification step. Nitrogen plasma MC-MICAP-MS technology circumvents Ar-related polyatomic interference generation at the ion source and permits routine low-resolution determination of Fe isotope ratios after automated purification. The current bottleneck is how to make the best decision on the least intensive preparation needed for each particular sample, so that the requirements in terms of isotope ratio accuracy and expanded uncertainties are met. The uncertainty-based approach towards a decision-making tool, based on validation of the maximum tolerances for Fe, Ca, K, Na, and Mg, alongside procedural blank, Fe recovery, instrument stability, control of Cr/Ni ratios, and mass-dependence isotope pairs, provides the Purification Necessity Index (PNI). According to the PNI, Fe samples are assigned to either direct Fe measurement, verifiable measurement, or Fe measurement after dual-column chromatographic purification. Based on nitrogen plasma Fe isotope validation data, it is found that formation of  $\text{CaN}^+$  and  $\text{KN}^+$  sets stringent limits on matrix effects, while Na and Mg have looser limits for the range of tested matrices/Fe levels. The analysis of results obtained with a set of reference materials proves  $\delta^{57}\text{Fe}/^{54}\text{Fe}_{\text{IRMM014}} - \delta^{56}\text{Fe}/^{54}\text{Fe}_{\text{IRMM014}}$  as an effective tool for internal checks of non-mass-dependent deviations. The developed matrix tolerance model for Fe biological materials, environmental waters, and transient-signal isotope-metallomics applications.

**Keywords:** iron isotopes; nitrogen plasma; MC-MICAP-MS; matrix effects; automated purification; uncertainty budget; isotope metallomics; route selection

## 1. Introduction

Stable iron isotope abundance ratios provide sensitive tracers of Fe sources, redox transformation, biological uptake, trophic transfer, and metallomic regulation because Fe occurs in multiple oxidation states and coordination environments across geological, environmental, and biological systems [1, 2, 3, 4]. The natural variability of  $^{56}\text{Fe}/^{54}\text{Fe}$  and  $^{57}\text{Fe}/^{54}\text{Fe}$  is analytically demanding: per mille-scale variations can be meaningful, and many environmentally or physiologically rel-

evant differences are smaller than the bias introduced by unresolved matrix effects. Reliable interpretation therefore requires high precision, demonstrable accuracy, and transparent control of spectral and non-spectral interferences [5, 6, 7].

Multi-collector inductively coupled plasma mass spectrometry (MC-ICP-MS) is the established technique for high-precision Fe isotope measurement [8, 1]. Argon-plasma instruments, however, encounter Ar-based molecular ions, especially  $^{40}\text{Ar}^{16}\text{O}^+$  on  $^{56}\text{Fe}^+$ , together with matrix-derived molecular species and isobaric overlaps such as

**Cite as:** D. H. Waldeck (2026). Uncertainty-Aware Matrix-Tolerance Decision Model for Direct and Automated Iron Isotope Analysis by Nitrogen-Plasma MC-MICAP-MS. LC GC Eu., 39(1) (2026) 23-29.



This work is licensed under Creative Commons Attribution-NonCommercial 4.0 International License

$^{54}\text{Cr}^+$  on  $^{54}\text{Fe}^+$  and  $^{58}\text{Ni}^+$  on  $^{58}\text{Fe}^+$  [8, 9, 10]. High mass resolution, cold-plasma operation, collision/reaction-cell strategies, and extensive chemical purification can address these problems, but each approach adds operational complexity, reduces sensitivity, increases preparation time, or raises the risk of blank and recovery losses [11, 12, 13].

A nitrogen-sustained microwave inductively coupled atmospheric-pressure plasma offers a complementary strategy by eliminating Ar-derived interferences before ion extraction. Recent MC-MICAP-MS applications have demonstrated accurate Ca and Sr isotope measurement and reliable Fe isotope measurement after automated dual-column purification [14, 15]. For Fe, published validation experiments show intermediate precision of 0.07‰ for  $\delta^{56}\text{Fe}/^{54}\text{Fe}_{\text{IRMM014}}$  and 0.13‰ for  $\delta^{57}\text{Fe}/^{54}\text{Fe}_{\text{IRMM014}}$ , negligible  $\text{CaN}^+$  and  $\text{KN}^+$  effects below approximately  $\text{Ca}/\text{Fe} \leq 0.01$  and  $\text{K}/\text{Fe} < 0.1$ , and substantial tolerance to Na and Mg up to matrix/Fe ratios of one [15]. Low procedural blank, high Fe recovery, and agreement between processed reference materials and literature values confirm the analytical potential of nitrogen-plasma Fe isotope measurement.

However, such characteristics alone do not necessarily provide criteria for the optimal sample preparation procedure. Complete sample purification may become necessary, should the content of Ca, K, Cr, Ni, blank fraction, or recovery exceed the defined tolerance; nevertheless, complete purification for all samples is an excessive measure leading to higher acid use, larger quantities of resin needed, increased preparation time, and greater risk of losses and contamination. At the same time, direct determination of isotope ratio without acceptance criteria may result in unidentified isotope effect. Hence, the question arises not whether purification is useful, but how much is necessary for a specific matrix and Fe mass while targeting a certain accuracy of measurement. The presented method of determining the necessity of sample purification could thus be considered a metrological rather than procedural choice. Four main contributions are included in the analysis: conversion of tolerance limits of impurity elements into a set of normalized scores corresponding to the spectral and non-spectral matrix; the requirement for both the blank level and the recovery ratio to be below a threshold, ensuring that the low-Fe samples will not be selected based on the matrix ratios alone; obligatory quality control for instrumental stability and Cr/Ni levels; and the utilization of the expected mass-dependent relation between  $\delta^{57}\text{Fe}/^{54}\text{Fe}_{\text{IRMM014}}$  and  $\delta^{56}\text{Fe}/^{54}\text{Fe}_{\text{IRMM014}}$ . This leads to the concept of the Purification Necessity Index (PNI), which helps classify samples for direct measurement, verification-limited measurement, or dual-column purification.

## 2. Materials and methods

### 2.1. Analytical basis and validation data

The decision model was parameterized from validation experiments for Fe isotope analysis by nitrogen-plasma MC-MICAP-MS with automated dual-column purification [15]. The validation basis includes repeated measurements of Fe-ICP and IRMM014 solutions, Ca, K, Na, and Mg matrix-addition tests, procedural blank and recovery determinations, processed IRMM014 experiments for evaluating on-column fractionation, and biological and environmental reference-material measurements. These measurements directly constrain the principal error sources relevant to nitrogen-plasma Fe isotope analysis: matrix-derived molecular ions, non-spectral matrix response, blank contribution, recovery-related fractionation, and mass-dependent isotope-ratio behavior.

The model uses the residual or pre-purification mass-concentration ratios  $\text{Ca}/\text{Fe}$ ,  $\text{K}/\text{Fe}$ ,  $\text{Na}/\text{Fe}$ , and  $\text{Mg}/\text{Fe}$ , together with Fe mass, procedural blank, Fe recovery, standard stability, and paired  $\delta^{56}\text{Fe}/^{54}\text{Fe}_{\text{IRMM014}}$  and  $\delta^{57}\text{Fe}/^{54}\text{Fe}_{\text{IRMM014}}$  values. When run-level data are available, the same equations can be applied to individual samples. When only upper-bound screening values are available, the

classification remains conservative because the largest plausible matrix contribution is used. Screening measurements by quadrupole ICP-MS are adequate for assigning route class when calibration, dilution, and matrix matching are documented.

The validation logic uses three independent checks. Matrix tolerance evaluates whether residual elements can produce molecular or non-spectral bias. Chemical preparation integrity evaluates whether blank and recovery are compatible with sample Fe mass and the target uncertainty. Isotope-ratio self-consistency evaluates whether the measured  $\delta^{57}\text{Fe}/^{54}\text{Fe}_{\text{IRMM014}}/\delta^{56}\text{Fe}/^{54}\text{Fe}_{\text{IRMM014}}$  pair follows mass-dependent fractionation within the combined expanded uncertainty. A sample route is accepted only when these checks give a consistent analytical interpretation.

### 2.2. Isotope notation and uncertainty target

Iron isotope results are expressed in delta notation relative to IRMM014. With  $R_{x/54} = {}^x\text{Fe}/^{54}\text{Fe}$ ,

$$\delta^x\text{Fe}/^{54}\text{Fe}_{\text{IRMM014}} = \left[ \frac{R_{x/54}^{\text{sample}}}{R_{x/54}^{\text{IRMM014}}} - 1 \right] \times 1000, \quad (1)$$

$$x \in \{56, 57\}.$$

For route selection, the observed isotope value is written as the sum of true isotope composition, matrix-dependent bias, instrumental mass-bias residual, blank contribution, recovery-related bias, and random measurement error:

$$\delta_{x,\text{obs}} = \delta_{x,\text{true}} + B_{x,\text{matrix}} + B_{x,\text{inst}} + B_{x,\text{blank}} + B_{x,\text{recovery}} + \epsilon_x. \quad (2)$$

An analytical route is acceptable when the combined systematic contribution remains smaller than the expanded uncertainty allowed for the scientific interpretation:

$$P\{|B_{x,\text{matrix}} + B_{x,\text{inst}} + B_{x,\text{blank}} + B_{x,\text{recovery}}| > U_x^*\} \leq \alpha. \quad (3)$$

Here,  $U_x^*$  denotes the maximum allowable expanded uncertainty or bias, and  $\alpha$  is the laboratory-defined tolerance for accepting an unrecognized systematic contribution. For the natural-abundance Fe isotope applications considered,  $U_{56}^*$  is taken as 0.07‰, matching the expanded intermediate precision reported for  $\delta^{56}\text{Fe}/^{54}\text{Fe}_{\text{IRMM014}}$ ; stricter applications can reduce this value without changing the route-selection equations.

### 2.3. Matrix-risk functions

Element-specific tolerance limits are expressed as normalized scores. For element  $e$ , with measured mass-concentration ratio  $e/\text{Fe}$  and tolerance limit  $T_e$ ,

$$S_e = \frac{e/\text{Fe}}{T_e}. \quad (4)$$

The adopted tolerance limits are

$$\begin{aligned} T_{\text{Ca}} &= 0.01, & T_{\text{K}} &= 0.1, \\ T_{\text{Na}} &= 1, & T_{\text{Mg}} &= 1. \end{aligned} \quad (5)$$

The spectral-interference score and non-spectral matrix score are then

$$\begin{aligned} S_{\text{spec}} &= \max(S_{\text{Ca}}, S_{\text{K}}), \\ S_{\text{matrix}} &= \max(S_{\text{Na}}, S_{\text{Mg}}). \end{aligned} \quad (6)$$

This separation is required because Ca and K primarily control nitrogen-plasma molecular overlap, whereas Na and Mg mainly test

**Table 1:** Published validation constraints used to parameterize the uncertainty-aware matrix-tolerance decision model.

Analytical component	Constraint used in decision model	Implication for route selection
Intermediate precision, $\delta^{56}\text{Fe}/^{54}\text{Fe}_{\text{IRMM014}}$	0.07‰ (2 SD)	Expanded precision target for the principal isotope ratio.
Intermediate precision, $\delta^{57}\text{Fe}/^{54}\text{Fe}_{\text{IRMM014}}$	0.13‰ (2 SD)	Expanded precision target for the secondary isotope ratio and consistency gate.
Ca-derived interference	$\text{Ca}/\text{Fe} \leq 0.01$	$\text{CaN}^+$ contribution is negligible below this limit under validated conditions.
K-derived interference	$\text{K}/\text{Fe} < 0.1$	$\text{KN}^+$ contribution is negligible below this limit under validated conditions.
Na matrix effect	$\text{Na}/\text{Fe} \leq 1$	No resolvable non-spectral effect within the tested range.
Mg matrix effect	$\text{Mg}/\text{Fe} \leq 1$	No resolvable non-spectral effect within the tested range.
Procedural blank	Approximately $2.4 \pm 2.0$ ng Fe	Blank contribution should remain below 1% of sample Fe mass unless blank composition is corrected.
Fe recovery	Approximately quantitative; near $99 \pm 8\%$	Recovery close to unity indicates low risk of on-column isotope fractionation.
Processed IRMM014 offset	$\Delta_{56} = -0.02 \pm 0.05\%$ ; $\Delta_{57} = 0.00 \pm 0.12\%$	Automated purification does not produce a resolvable isotope offset.
Mass-dependent behavior	Slope $1.489 \pm 0.001$ ; theoretical value 1.488	The isotope-pair relation can identify non-mass-dependent analytical offsets.

non-spectral matrix tolerance. Chromium and nickel are treated as exclusionary monitors rather than continuous risk terms because the relevant isobaric overlaps on  $^{54}\text{Fe}^+$  and  $^{58}\text{Fe}^+$  cannot be resolved by mass resolution in the stated collector geometry. If  $^{53}\text{Cr}^+$  or  $^{60}\text{Ni}^+$  monitor signals exceed laboratory correction limits, full purification or validated mathematical correction is required.

#### 2.4. Blank, recovery, and instrumental-stability scores

The blank score is normalized to a one-percent contribution threshold:

$$S_{\text{blank}} = \frac{m_{\text{blank}}}{0.01 m_{\text{Fe}}}, \quad (7)$$

where  $m_{\text{blank}}$  is procedural Fe blank and  $m_{\text{Fe}}$  is the Fe mass loaded or measured. The threshold can be tightened when blank isotope composition is poorly constrained or when sample isotope composition is expected to approach the blank value.

Recovery risk is defined as

$$S_{\text{rec}} = \frac{|R - 1|}{T_R}, \quad T_R = 0.15, \quad (8)$$

where  $R$  is fractional Fe recovery. The tolerance  $T_R = 0.15$  is conservative for automated methods that show no measurable on-column isotope fractionation at near-quantitative recovery. Recovery outside this interval does not prove isotope bias, but it requires verification because incomplete recovery can matter when the retained and lost fractions are isotopically different.

Instrumental stability is imposed as a binary gate. A sequence is accepted only when standard-sample bracketing remains within intermediate-precision limits, analyte concentration matching is documented, signal intensity is stable, and laboratory temperature variation remains within validated operating conditions. Failure of any stability condition requires repetition of the sequence, uncertainty inflation supported by control measurements, or reassignment to a more conservative route.

#### 2.5. Purification Necessity Index

The Purification Necessity Index is defined as

$$\text{PNI} = \max(S_{\text{spec}}, S_{\text{matrix}}, S_{\text{blank}}, S_{\text{rec}}), \quad (9)$$

subject to acceptable Cr/Ni monitoring and a passed instrumental-stability gate. Route class is assigned as

$$\text{route} = \begin{cases} \text{A}, & \text{PNI} \leq 0.5, \\ \text{B}, & 0.5 < \text{PNI} \leq 1.0, \\ \text{C}, & \text{PNI} > 1.0. \end{cases} \quad (10)$$

The boundary at  $\text{PNI} = 1$  corresponds to at least one validated tolerance limit being reached. The lower boundary at  $\text{PNI} = 0.5$  supplies a guard band because single-element addition tests do not fully capture mixed-matrix behavior, acid mismatch, organic residues, or transient ionization effects. Direct or minimally purified measurement is therefore assigned only when chemical scores, blank and recovery scores, instrumental stability, Cr/Ni monitors, and isotope-pair consistency support the same conclusion.

#### 2.6. Mass-dependent isotope consistency gate

Published nitrogen-plasma Fe isotope measurements follow mass-dependent behavior consistent with the exponential law, with a measured three-isotope slope of approximately 1.489 and a theoretical value near 1.488. The measured  $\delta^{57}\text{Fe}/^{54}\text{Fe}_{\text{IRMM014}}$  value can therefore be compared with the value predicted from  $\delta^{56}\text{Fe}/^{54}\text{Fe}_{\text{IRMM014}}$ :

$$D_{57/56} = \delta^{57}\text{Fe}/^{54}\text{Fe}_{\text{IRMM014}} - \beta \delta^{56}\text{Fe}/^{54}\text{Fe}_{\text{IRMM014}}, \quad (11)$$

$$\beta = 1.488.$$

The expanded-uncertainty-normalized consistency statistic is

$$Z_{57/56} = \frac{D_{57/56}}{U_{57/56}}, \quad (12)$$

$$U_{57/56} = \left( U_{57}^2 + \beta^2 U_{56}^2 \right)^{1/2}.$$

where  $U_{56}$  and  $U_{57}$  are expanded uncertainties for  $\delta^{56}\text{Fe}/^{54}\text{Fe}_{\text{IRMM014}}$  and  $\delta^{57}\text{Fe}/^{54}\text{Fe}_{\text{IRMM014}}$ . Measurements with  $|Z_{57/56}| \leq 1$  agree within the combined expanded uncertainty, while  $1 < |Z_{57/56}| \leq 2$  is retained as a review interval that requires all independent matrix, blank, recovery, and stability gates to pass. Values outside this interval indicate possible unresolved interference, matrix mismatch, blank contribution, correction error, or sequence instability, even when  $\delta^{56}\text{Fe}/^{54}\text{Fe}_{\text{IRMM014}}$  alone appears precise.

### 3. Results

#### 3.1. Matrix tolerance defines measurable route boundaries

The tolerance limits for Ca, K, Na, and Mg divide route selection into spectral and non-spectral components. Calcium and potassium provide the strictest constraints because they form nitrogen-plasma molecular ions that can overlap Fe isotope masses. Sodium and magnesium are less restrictive under the validated conditions, with no resolvable

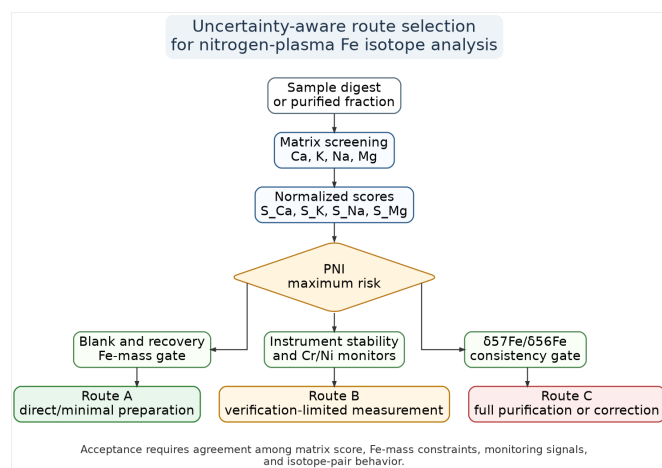


**Figure 1:** Analytical decision sequence for uncertainty-aware route selection in nitrogen-plasma Fe isotope analysis. Matrix screening, Fe-mass constraints, instrumental monitoring, and isotope-pair consistency are evaluated before assigning a preparation route.

**Table 2:** Analytical route classes assigned by the Purification Necessity Index.

Class	Criterion	Analytical action
Route A	$PNI \leq 0.5$	Direct or minimally purified measurement is acceptable only when Cr/Ni monitors are within limits and $ Z_{57/56}  \leq 2$ . This route is suited to low-matrix fractions, clean environmental waters after concentration, and validated hyphenated workflows.
Route B	$0.5 < PNI \leq 1.0$	Measurement requires verification by replicate matrix-matched standards, dilution, standard addition, repeated bracketing, or partial purification. Matrix ratios used for acceptance should be reported with the isotope results.
Route C	$PNI > 1.0$	Full dual-column purification, separation redesign, or validated mathematical correction is required. This route is mandatory when Ca/K spectral risk, Cr/Ni interference, blank contribution, or recovery risk exceeds acceptance limits.

isotope effect up to matrix/Fe ratios of one. This asymmetry is analytically important: a sample may contain tolerable Na and Mg but still require purification because the  $\text{CaN}^+$  or  $\text{KN}^+$  risk exceeds the allowable Ca/K spectral window.

Figure 2 shows the most restrictive portion of the route-selection space. The lower-left region is the only Ca/K domain in which direct or minimally purified measurement is chemically plausible. The upper-right region requires full purification because both  $\text{CaN}^+$  and  $\text{KN}^+$  risks exceed the validated tolerance space. The two off-diagonal regions have a single dominant spectral risk and therefore require verification by matrix-matched standards, replicate dilution, standard addition, or targeted partial removal before isotope values can be accepted.

### 3.2. The Purification Necessity Index assigns route classes

Table 2 summarizes the route classes. The index distinguishes samples with a broad safety margin from samples that merely remain below a single tolerance limit. This distinction is necessary because real digests may contain combined matrices, acid residues, organic components, and instrument-state effects not represented by single-element addition tests. The interval  $0.5 < PNI \leq 1.0$  is therefore interpreted as a verification zone rather than as an automatic rejection zone.

### 3.3. Blank and recovery constraints protect low-Fe samples

The automated dual-column purification procedure achieved low procedural blanks and near-quantitative recovery, making it suitable for

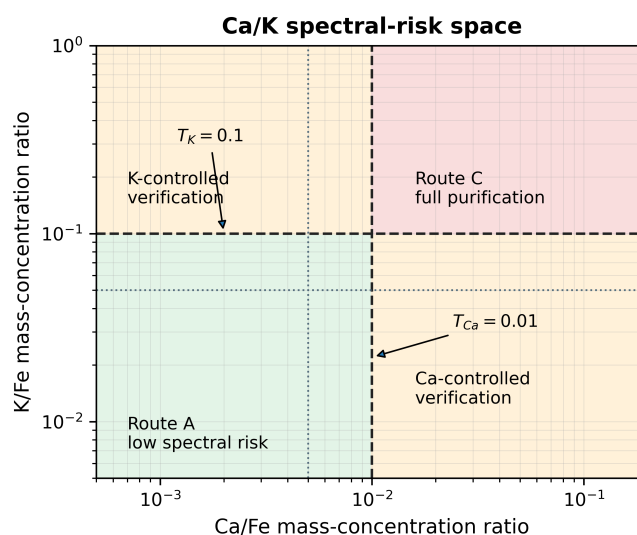


**Figure 2:** Ca/K spectral-risk space for nitrogen-plasma Fe isotope analysis. Dashed boundaries indicate the validated tolerance limits  $\text{Ca/Fe} = 0.01$  and  $\text{K/Fe} = 0.1$ ; dotted boundaries indicate the route-A guard band at half of each limit. Values below both tolerance limits must also satisfy blank, recovery, stability, Cr/Ni monitoring, and mass-dependent consistency requirements.

limited biological and environmental materials. The blank term nevertheless becomes decisive as Fe mass decreases. Using Eq. (7), a 2.4 ng blank contributes 0.24% to a 1000 ng Fe load and 0.48% to a 500 ng load; both values are below the one-percent threshold. At 250 ng Fe, the same blank approaches the threshold, and a conservative upper blank estimate of 4.4 ng reaches one percent at approximately 440 ng Fe. The lower practical Fe mass limit is therefore controlled not by sensitivity alone, but by blank fraction, blank isotope composition, and the uncertainty target.

Recovery acts through a different mechanism. Recovery near unity reduces the risk of chromatographic isotope fractionation. Processing IRMM014 through the automated purification procedure produced no resolvable offset within uncertainty, supporting full automated purification as the reference route. In the present model, recovery between approximately 85% and 115% is acceptable for routine route selection. Values outside this interval require verification even when the measured isotope ratio is precise, because precision alone cannot exclude incomplete chemical recovery.

### 3.4. Mass-dependent consistency provides an internal isotope-ratio quality gate

The  $\delta^{57}\text{Fe}/^{54}\text{Fe}_{\text{IRMM014}}$  reference material ratios were tested against the calculated ratios from  $\delta^{56}\text{Fe}/^{54}\text{Fe}_{\text{IRMM014}}$  with  $\beta = 1.488$ . This data set is provided in Table 3, along with a graphical representation of the results in Figure 3. All the reference materials meet  $|Z_{57/56}| \leq 2$  and five out of six are within the expanded-uncertainty confidence interval. NIST SRM 1400 has the highest normalized residual, but the isotope pair is still within acceptable limits and can be further investigated under low tolerance application conditions. These reference materials include mineral, biological, and aqueous matrices, such as bone ash, bovine liver, human hair, and river water. This indicates the utility of  $\delta^{57}\text{Fe}/^{54}\text{Fe}_{\text{IRMM014}}$  as both a secondary isotope ratio and quality control parameter for offset analysis.

### 3.5. Reporting requirements for method transfer

For transfer between laboratories, isotope results should be reported with the variables that determine route class. A complete report should

**Table 3:** Mass-dependent consistency test for biological and environmental reference materials. Values use published isotope results and expanded uncertainties.

Reference material	$\delta^{56}\text{Fe}/^{54}\text{Fe}_{\text{IRMM014}}$	$U_{56}$ (‰)	$\delta^{57}\text{Fe}/^{54}\text{Fe}_{\text{IRMM014}}$	$U_{57}$	$Z_{57/56}$
NIST SRM 1400 (bone ash)	0.06	0.07	0.31	0.15	1.21
NIST SRM 1577c (bovine liver)	-1.36	0.09	-2.02	0.14	0.02
GBW07601 (human hair)	-0.14	0.07	-0.16	0.13	0.29
GBW09101 (human hair)	-0.06	0.07	-0.03	0.13	0.36
ERM-DB001 (human hair)	-0.49	0.12	-0.73	0.19	0.00
SLRS-6 (river water)	0.44	0.14	0.72	0.25	0.20

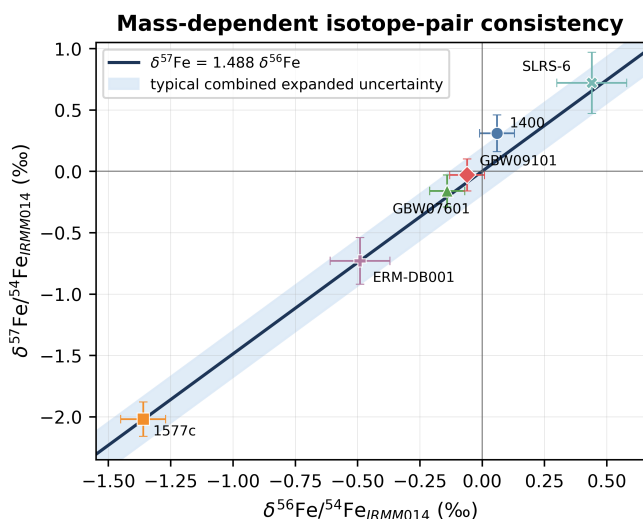


**Figure 3:** Reference-material isotope-pair consistency for the mass-dependent gate. Points show paired  $\delta^{56}\text{Fe}/^{54}\text{Fe}_{\text{IRMM014}}$  and  $\delta^{57}\text{Fe}/^{54}\text{Fe}_{\text{IRMM014}}$  values with expanded uncertainties; the solid line is the theoretical mass-dependent relation  $\delta^{57}\text{Fe}/^{54}\text{Fe}_{\text{IRMM014}} = 1.488\delta^{56}\text{Fe}/^{54}\text{Fe}_{\text{IRMM014}}$ , and the shaded band indicates a typical combined expanded uncertainty.

include Fe mass processed, procedural blank, Fe recovery, residual Ca/Fe, K/Fe, Na/Fe, and Mg/Fe, Cr and Ni monitor signals or correction status, standard concentration matching, bracketing stability, temperature stability,  $\delta^{56}\text{Fe}/^{54}\text{Fe}_{\text{IRMM014}}$ ,  $\delta^{57}\text{Fe}/^{54}\text{Fe}_{\text{IRMM014}}$ , expanded uncertainties,  $Z_{57/56}$ , PNI, and selected route. Figure 4 summarizes the reporting logic. These variables distinguish results supported by matrix removal from results supported by demonstrated matrix tolerance and isotope-pair consistency, and they allow readers to evaluate whether simplified preparation was justified for the reported uncertainty.

## 4. Discussion

### 4.1. From fixed preparation to evidence-based route selection

Fe isotope methods are typically validated to ensure accurate results with standards and reference materials using a specified preparation and analytical procedure. This is an essential part of the process, but it does not establish whether this level of chemical purification will always be necessary in practice. The decision model moves from a fixed procedure to an evaluation of the actual chemical and instrumental state of the given sample. This change is especially relevant to MC-MICAP-MS as the lack of Ar-derived interference eliminates a major impediment, but some matrix-related risks remain. The key aspect of the model lies in its ability to separate four criteria that are often combined in routine method application. Are Ca and K low enough to exclude potential molecular nitrogen interference? Are Na and Mg low enough to rule out non-spectral matrix effects? Is

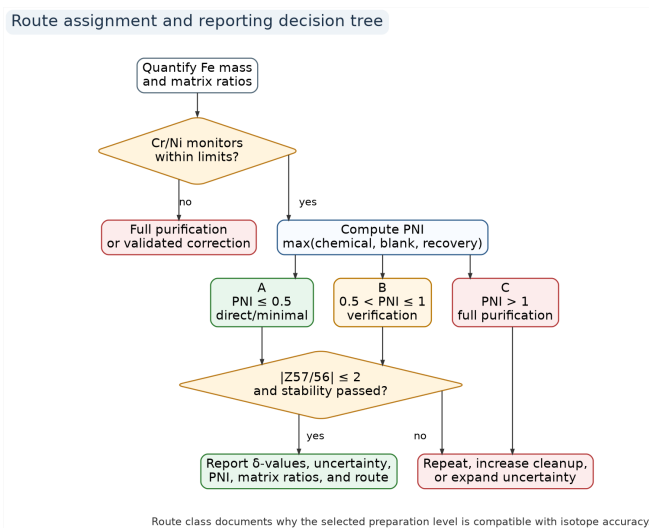


**Figure 4:** Decision tree for route assignment and result reporting. The reporting sequence links matrix screening, Cr/Ni monitoring, PNI class, instrumental stability, and isotope-pair behavior before isotope values are accepted.

blank and recovery within the required range compared to Fe content and mass uncertainty target? Does the measured isotope pair follow mass-dependent behavior? Simplified purification should only occur when all four requirements are fulfilled.

### 4.2. Why Ca and K are the key residual matrix elements

According to the decision model, Ca and K are the main residual elements affecting the analysis of Fe isotope ratios by nitrogen plasma. This conclusion is explained by their ability to form molecular ions ( $\text{Ca}^+$  and  $\text{KN}^+$ ) and their more stringent tolerance limits compared to Na and Mg. In biological or environmental materials, Ca and K are usually unrelated to Fe content. Consequently, bone-enriched samples, high-carbonate waters, or plant-derived samples may require full or partial Ca/K depletion even when Na and Mg are within tolerances. The model prevents overstatement of single-element matrix tolerance as well. For example,  $\text{Na}/\text{Fe} \leq 1$  indicates that Na was low enough so that it did not cause an observable offset in isotopic measurements. It does not mean that any digest can be measured directly since combined effects, acid residue, organic impurities, or high total dissolved solids may lead to altered nebulization, ion extraction, or mass-bias characteristics. The guard band ( $\text{PNI} = 0.5$ ) takes these risks into account and requires additional validation prior to approval.

### 4.3. Mass-dependent self-consistency as a quality control tool

The simultaneous analysis of both  $^{56}\text{Fe}/^{54}\text{Fe}$  and  $^{57}\text{Fe}/^{54}\text{Fe}$  allows testing the consistency of the mass-dependent pattern for each sample. While the  $\delta^{57}\text{Fe}/^{54}\text{Fe}_{\text{IRMM014}}/\delta^{56}\text{Fe}/^{54}\text{Fe}_{\text{IRMM014}}$  relationship cannot substitute for chemical purification, it can highlight any non-mass dependent interference that causes an observed isotopic difference between two isotopes.  $\text{CaN}^+$ ,  $\text{KN}^+$ , blank, mismatched matrix, or Cr/Ni addition can create this kind of effect. Normalized parameter  $Z_{57/56}$  turns this test into a quantifiable indicator.

All considered isotope pairs of reference materials lie inside the accepted mass-dependent range, which supports the reliability of the gate for the selected materials. It does not mean, however, that there is no uncertainty about the gate. For samples with low  $\delta^{56}\text{Fe}/^{54}\text{Fe}_{\text{IRMM014}}$  values, the expected  $\delta^{57}\text{Fe}/^{54}\text{Fe}_{\text{IRMM014}}$  prediction can fall within the expanded uncertainty interval, resulting in a low discriminatory power. In such cases, matrix screening, Cr/Ni monitoring, blank correction,

and bracketing stability become crucial factors to consider.

#### 4.4. Practical implications for high-throughput and low-mass isotope metallomics

Decision-making in MC-MICAP-MS becomes especially valuable for high-throughput and low-mass isotope analysis. Many applications of isotope metallomics use small biological samples or limited clinical samples. Environmental monitoring involves large numbers of water samples containing different concentrations of Fe and matrix. Hyphenated analysis with LC-ICPMS or LA-ICPMS generates time-dependent signals with which off-line purification is unfeasible. Full sample preparation is not efficient for these situations, but direct measurements without the gates are analytically unreasonable.

The proposed route selection framework offers an effective solution in such cases. Direct, partially purified, or fully purified measurements are possible depending on the chemical and instrumental factors evaluated collectively. This allows minimizing unnecessary sample manipulation without compromising the conservative rationale behind isotope ratio measurements. Moreover, this model facilitates the transferability of methods, since it defines the route of analysis based on clear criteria rather than subjective assessment of the analyst.

#### 4.5. Limitations and laboratory validation requirements

The developed model relies on conservative criteria, as it uses average validated figures and matrix tolerance determined through single-element additions. More detailed laboratory validation must employ factorial experimental design to find out if matrix effects are additive, independent, or interactive. It should test acid residue effects, total dissolved solids, organic residue, signal transient introduction, concentration mismatch, daily temperature variations, etc. The PNI should be used as a route selection and reporting instrument whose threshold values can be fine-tuned with more replicates.

Clinical, forensic, or regulatory applications require laboratory-specific validation using certified reference materials, quality control solutions, blanks, duplicates, inter-laboratory calibration, etc. Such tests establish the exact conditions for performing simplified sample purification. Any deviation from these conditions implies the necessity of full or partial purification according to the decision model.

## 5. Conclusions

While nitrogen plasma removes Ar interference, it preserves high accuracy, stability, and mass-independent behavior in Fe isotope analysis. Yet, the key analytical question still remains open. What kind of sample preparation is necessary for a particular matrix and uncertainty target? The uncertainty-aware matrix tolerance decision model helps answer this question by taking into account several risk factors such as CaN<sup>+</sup>, KN<sup>+</sup>, tolerance limits for Na/Mg, blank and recovery, instrumental instability, Cr/Ni presence, and mass-dependence of isotope pair.

The Purification Necessity Index introduces a formal approach to choosing a purification route: direct or minimally purified measurements, verification limited measurements, and full sample preparation. Based on this model, it is found that Ca and K are the primary matrix risk elements for MC-MICAP-MS within the tested matrix range, while Na and Mg are more relaxed in their tolerances. Also, the ratio  $\frac{\Delta^{57}\text{Fe}}{\Delta^{56}\text{Fe}}$  becomes a practical internal QC criterion.

By providing a quantitative, explicit, and reportable solution to the problem of route selection, the presented model enables rational use of automated chemical purification. This can help optimize isotope metallomics and high-throughput environmental studies involving small samples.

## References

- [1] Dauphas, N., John, S. G., & Rouxel, O. (2017). Iron isotope systematics. In F.-Z. Teng, J. Watkins, & N. Dauphas (Eds.), *Non-traditional stable isotopes* (pp. 415–510). De Gruyter.
- [2] Wiederhold, J. G. (2015). Metal stable isotope signatures as tracers in environmental geochemistry. *Environmental Science & Technology*, *49*, 2606–2624.
- [3] Irrgeher, J., & Prohaska, T. (2016). Application of non-traditional stable isotopes in analytical ecogeochemistry assessed by MC ICP-MS: A critical review. *Analytical and Bioanalytical Chemistry*, *408*, 369–385.
- [4] Mahan, B., Chung, R. S., Pountney, D. L., Moynier, F., & Turner, S. (2020). Isotope metallomics approaches for medical research. *Cellular and Molecular Life Sciences*, *77*, 3293–3309.
- [5] Jaouen, K., Pons, M.-L., & Balter, V. (2013). Iron, copper and zinc isotopic fractionation up mammal trophic chains. *Earth and Planetary Science Letters*, *374*, 164–172.
- [6] Guo, R., Yu, H.-M., Fang, S.-B., Xiao, Z.-C., & Huang, F. (2023). Iron, copper and zinc isotope compositions of biological reference materials determined by MC-ICP-MS. *Journal of Analytical Atomic Spectrometry*, *38*, 2365–2377.
- [7] Vanhaecke, F., & Costas-Rodriguez, M. (2020). High-precision isotopic analysis of essential mineral elements: Capabilities as a diagnostic/prognostic tool. *VIEW*, *2*, e202000094.
- [8] Weyer, S., & Schwieters, J. B. (2003). High precision Fe isotope measurements with high mass resolution MC-ICPMS. *International Journal of Mass Spectrometry*, *226*, 355–368.
- [9] Lei, Y., Li, M., Wang, Z., Zhu, Y., Hu, Z., Liu, Y., & Chai, X. (2022). Iron isotopic measurement using large-geometry high-resolution multi-collector inductively coupled plasma mass spectrometer. *Atomic Spectroscopy*, *43*, 214–222.
- [10] Chen, K.-Y., Yuan, H.-L., Liang, P., Bao, Z.-A., & Chen, L. (2017). Improved nickel-corrected isotopic analysis of iron using high-resolution multi-collector inductively coupled plasma mass spectrometry. *International Journal of Mass Spectrometry*, *421*, 196–203.
- [11] Chen, K., Bao, Z., Yuan, H., & Lv, N. (2022). Direct measurement of Fe isotope compositions in iron-dominated minerals without column chromatography using MC-ICP-MS. *Journal of Analytical Atomic Spectrometry*, *37*, 249–263.
- [12] Yang, K., Zhang, H., Zhou, J., Ying, Q., Zhou, S., Cheng, Y., Wei, X., Gu, X., Xia, Q., & Liu, J. (2025). High-precision Fe isotope analysis for low contents using a Nu Sapphire instrument. *Journal of Analytical Atomic Spectrometry*, *40*, 2418–2425.
- [13] Yang, W., You, C., Qiu, X., Tong, X., Lu, S., Duan, G., Cai, Y., Deng, H., & Yang, H. (2026). An improved single-column separating procedure of copper, iron, and zinc from geological samples for their isotopic measurements by MC-ICP-MS. *International Journal of Mass Spectrometry*, *522*. Advance online publication.
- [14] Retzmann, A., & Wieser, M. E. (2026). Advancing Ca isotopic analysis: Direct measurement of (<sup>44</sup>Ca/<sup>40</sup>Ca) isotopic composition by MC-MICAP-MS with nitrogen plasma. *Analytica Chimica Acta*, *1383*. Advance online publication.
- [15] Retzmann, A., Dubois Recinos, H. M., & Wieser, M. E. (2026). Nitrogen plasma meets automated purification: Direct and reliable Fe isotopic analysis with MC-MICAP-MS. *Analytica Chimica Acta*, *1414*, 345677.
- [16] Brand, W. A., Coplen, T. B., Vogl, J., Rosner, M., & Prohaska, T. (2014). Assessment of international reference materials for isotope-ratio analysis: IUPAC technical report. *Pure and Applied Chemistry*, *86*, 425–467.
- [17] Marechal, C. N., Telouk, P., & Albarede, F. (1999). Precise analysis of copper and zinc isotopic compositions by plasma-source mass spectrometry. *Chemical Geology*, *156*, 251–273.
- [18] Vanhaecke, F., & Moens, L. (2004). Overcoming spectral overlap in isotopic analysis via single- and multi-collector ICP-mass spectrometry. *Analytical and Bioanalytical Chemistry*, *378*, 232–240.
- [19] Guan, Q., Sun, Y., Zhang, Z., Liu, X., An, Y., Liu, F., & Zhao, S. (2020). Determination of ( $\delta^{44/40}\text{Ca}$ ) and ( $\delta^{56/54}\text{Fe}$ ) in geological materials combined with a simplified method for their separation using a single TODGA resin column. *Geostandards and Geoanalytical Research*, *44*, 669–683.
- [20] Romaniello, S. J., Field, M. P., Smith, H. B., Gordon, G. W., Kim, M. H., & Anbar, A. D. (2015). Fully automated chromatographic purification of Sr and Ca for isotopic analysis. *Journal of Analytical Atomic Spectrometry*, *30*, 1906–1912.
- [21] Retzmann, A., Zimmermann, T., Pr<sup>o</sup>ffrock, D., Prohaska, T., & Irrgeher, J. (2017). A fully automated simultaneous single-stage separation of Sr, Pb, and Nd using DGA resin for the isotopic analysis of marine sediments. *Analytical and Bioanalytical Chemistry*, *409*, 5463–5480.
- [22] Zimmermann, T., Retzmann, A., Schober, M., Pr<sup>o</sup>ffrock, D., Prohaska, T., & Irrgeher, J. (2019). Matrix separation of Sr and Pb for isotopic ratio analysis of Ca-rich samples via an automated simultaneous separation procedure. *Spectrochimica Acta Part B: Atomic Spectroscopy*, *151*, 54–64.
- [23] Mahan, B. M., Wu, F., Dosseto, A., Chung, R., Schaefer, B., & Turner, S. (2020). SpinChem: Rapid element purification from biological and geological matrices via centrifugation for MC-ICP-MS isotope analyses: A case study with Zn. *Journal of Analytical Atomic Spectrometry*, *35*, 863–872.

- [24] Enge, T. G., Field, M. P., Jolley, D. F., Ecroyd, H., Kim, M. H., & Dosseto, A. (2016). An automated chromatography procedure optimized for analysis of stable Cu isotopes from biological materials. *Journal of Analytical Atomic Spectrometry*, *31*, 2023–2030.
- [25] Kidder, J. A., Voinot, A., Sullivan, K. V., Chipley, D., Valentino, M., Layton-Matthews, D., & Leybourne, M. (2020). Improved ion-exchange column chromatography for Cu purification from high-Na matrices and isotopic analysis by MC-ICPMS. *Journal of Analytical Atomic Spectrometry*, *35*, 776–783.
- [26] Retzmann, A., Miller, K. A., Mohamed, F. A. A., & Wieser, M. E. (2025). Reliable and precise Zn isotopic analysis of biological matrices using a fully automated dual-column purification procedure. *Analytical and Bioanalytical Chemistry*, *417*, 835–846.
- [27] Retzmann, A., Miller, K. A., Champagne, S., Gelinas, G., & Wieser, M. E. (2025). Fully automated dual-column purification procedure for Pb from biological materials for subsequent high-precision isotopic analysis. *Journal of Analytical Atomic Spectrometry*, *40*, 2783–2791.
- [28] Russell, W. A., Papanastassiou, D. A., & Tombrello, T. A. (1978). Ca isotope fractionation on the Earth and other solar system materials. *Geochimica et Cosmochimica Acta*, *42*, 1075–1090.
- [29] Joint Committee for Guides in Metrology. (2008). *Evaluation of measurement data: Guide to the expression of uncertainty in measurement*. JCGM 100:2008.
- [30] International Organization for Standardization. (2019). *Accuracy (trueness and precision) of measurement methods and results*. ISO 5725 series.